

Buckling and Post-Buckling Behavior of Steel and Laminated Composite Cylindrical Shells Subjected to External Pressure

Robab Naseri GHALGHACHI ^a, Neda FAZLALIPOUR ^a and Saeed Eyvazinejad FIROUZSALARI ^{b,1}

^aDepartment of Civil Engineering, Urmia University, Urmia, Iran

^bDepartment of Civil and Environmental Engineering, The University of Auckland, New Zealand

Abstract. Tanks are commonly used to store various petrochemical products, water, etc., and therefore are considered a strategic infrastructure type and vital for social functions. Tank structural failure can cause significant life and financial losses and severe environmental damage depending on the content material. Thin-walled cylindrical shells can structurally fail in the form of buckling if the loading exceeded the bearing capacity of the shells. FRP composites are a relatively modern construction material type. It has high stiffness and a high strength-to-weight ratio; therefore, FRP composites are also used for tank construction in addition to steel material. In this study, the buckling and post-buckling behaviour of steel and laminated carbon fibre composite (CFRP) cylindrical shells with different geometrical properties when subjected to uniform external pressure is studied numerically using Abaqus finite element software and Riks analysis. The results indicated that the buckling load of the shells decreased significantly with increasing the radius-to-thickness ratio (R/t) and radius-to-length ratio (R/L) of the cylindrical shells.

Keywords. Buckling behavior, uniform external pressure, steel and laminated composite shells, thin-walled cylindrical shells, CFRP Introduction

1. Introduction

The use of cylindrical shells in various forms, such as silos and tanks, for storing various materials has received substantial attention in different industrial sectors. Tanks typically have significantly smaller wall-thickness when compared to their height and diameter, which makes them susceptible to structural failure in the form of buckling [1,2]. Buckling failure of tanks containing liquids can result from various loading scenarios; however, uniform external pressure is considered the most prominent loading that causes tank buckling.

Several studies have been conducted on the buckling behaviour of thin-walled steel tanks under external pressure. Showkati and Ansourian [3] investigated the effect of support conditions on the buckling behaviour of steel cylindrical shells subjected to

¹ Saeed Eyvazinejad Firouzsalar, Corresponding Author, Department of Civil and Environmental Engineering, The University of Auckland, New Zealand; Email: seyv943@aucklanduni.ac.nz

uniform external pressure and proposed relationships to obtain the number of circumferential waves and buckling pressure. Fatemi et al. [4] investigated the effect of geometric imperfections on the buckling behavior of steel cylindrical shells with different length-to-radius ratio (L/R) and radius-to-thickness (R/t) ratios under external pressure. The results showed that shells with the lowest L/R and highest R/t ratios were less sensitive to geometric imperfections. Maali et al. [5] investigated the effect of longitudinal imperfections on the buckling and post-buckling behaviour of thin-walled cylindrical shells under uniform external pressure. The results indicated imperfections acted as stiffeners beyond a specific value, and the shell's buckling capacity increased. Pan and Liang [6] investigated the buckling behaviour of two 100,000 m³ open-roof tanks under external pressure using finite element (FE) simulations. The results showed that the critical buckling pressure obtained from the theoretical calculations based on Donnell's theory was close to the FE results, while the FE results were rather conservative. Yousefi and Showkati [7] experimentally investigated the buckling and post-buckling response of thin-walled steel cylindrical shells reinforced with CFRP rings under uniform external pressure. They reported that CFRP rings effectively increased the buckling capacity of thin-walled shells by changing the vertical buckling mode and increasing the circumferential waves against uniform external pressure. Zhang et al. [8] numerically and experimentally investigated the buckling capacity of composite cylindrical shells under hydrostatic pressure. The effect of parameters such as ply angle and stacking sequence, L/R ratio, and thickness-to-radius ratio (t/R) were evaluated. The results showed that the L/R ratio had little influence on the failure pressure of the shells. In contrast, the t/R ratio, ply angle and stacking sequence significantly influenced the critical buckling pressure of the shells. Wei et al. [9] investigated the delamination damage and the effect of buckling behaviour on the delamination propagation of the composite cylindrical shells subjected to hydrostatic pressure. The results showed that local or global buckling of the shell promoted the propagation of delamination, and the ultimate buckling pressure of the shell was more sensitive to the axial initial delamination length. Showkati and Pashaei [10] experimentally investigated the buckling and post-buckling behaviour of glass fibre-reinforced composite (GFRP) cylindrical shells with different L/R and R/t ratios under uniform external pressure. The results showed that with increasing the R/t ratio, the buckling capacity of the shells decreased, and the number of buckling modes increased. With increasing the R/L ratio, the buckling capacity of the shells increased, and the number of buckling modes decreased.

FRP composites are considered emerging materials in the construction sector. They have attracted substantial attention for use in various structure types, such as tank construction, mainly due to FRP composites' high strength-to-weight ratio and corrosion resistance characteristics. Therefore, it is crucial to investigate the behaviour of FRP composite shells when subjected to various loading types.

2. Finite Element Modeling

ABAQUS finite element program was used to develop three-dimensional nonlinear elastic-plastic finite element models for cylindrical shells subjected to uniform external pressure [11]. First, the cylindrical shell was modelled using a shell element (due to its minimal thickness compared to the length and radius). The characteristics of the steel and CFRP materials were modelled using the actual stress-strain values calculated from

the engineering stress-strain curve obtained from the tensile test coupon. The bottom edge of the cylindrical shell was constrained against vertical and radial displacements, and the top edge of the cylindrical shell was only constrained against radial displacements, with no rotational constraint considered at both the top and bottom edges (see figure 1) [12,13].

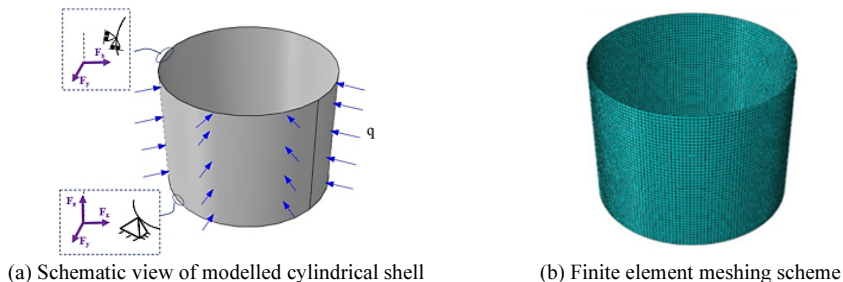


Figure 1. Details of finite element model.

The cylindrical shells were modelled using four-node, three-dimensional and doubly curved shell element S4R with three translational and three rotational degrees of freedom, which is suitable for analyzing large strains. Two analysis types were performed to investigate the cylindrical models' stability, including linear static eigenvalues and nonlinear Riks [14,15]. The load was applied to the external surface of the cylindrical shells in the form of uniform external pressure. Convergence and mesh refinement studies were performed to ensure high accuracy in the analysis in the shortest time.

3. Problems of Model

All cylindrical shells had the same radius of $R = 300$ mm but had different lengths of $L = 150, 455$ and 900 mm and different wall thicknesses. The L/R ratio for the shell models was 0.50, 1.50 and 3. For steel models, R/t was equal to 300, 500, 750, and 1000 and wall thickness was equal to 0.3, 0.4, 0.6, and 1 and for laminated composite models, the R/t ratio was equal to 100, 214 and 300 and wall thickness was equal 1, 2, and 3. The ply angle and the stacking sequence are considered 45/-45 and 0/90 (see figure 2).

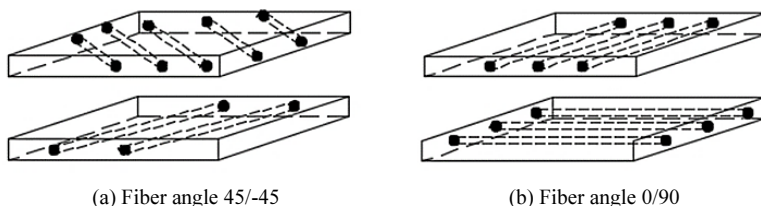


Figure 2. The ply angle and the stacking sequence of the models.

The geometric properties of the steel models are given in table 1, with each model identified with a code 'S-x-y' in which the subcode 'S' refers to steel models, 'x' refers

to R/t ratios and ‘y’ refers to L/R ratios. For instance, S-300-0.5 refers to a model with $R/t = 300$ and $L/R = 0.5$.

Table 1. Geometrical properties of steel cylindrical shell models.

Model	Length (mm)	Radius (mm)	Thickness (mm)
S-300-0.5	150	300	1.0
S-300-1.5	450	300	1.0
S-300-3	900	300	1.0
S-500-0.5	150	300	0.6
S-500-1.5	450	300	0.6
S-500-3	900	300	0.6
S-750-0.5	150	300	0.4
S-750-1.5	450	300	0.4
S-750-3	900	300	0.4
S-1000-0.5	150	300	0.3
S-1000-1.5	450	300	0.3
S-1000-3	900	300	0.3

Mild steel was used to model the cylindrical steel shells, with this steel type being considered bilinear elastoplastic with a modulus of elasticity of 200 GPa and a Poisson's ratio of 0.3. The mechanical properties of mild steel are given in table 2.

Table 2. Material specifications of mild steel.

Yielding stress (MPa)	Plastic strain
200	0.0
220	0.01
360	0.2

Table 3 shows the properties of the composite materials based on manufacturer standards. To evaluate the performance of composite materials, the linear elastic behaviour of undamaged materials was modelled based on Hashin's theory in four failure modes, including fibre tension, fibre compression, matrix tension, and matrix compression (see table 4). In ABAQUS, the damage initiation for fibre-reinforced materials depended on the point at which material stiffness degraded, with that damage evolution being characterised by progressive degradation of material stiffness leading to failure [16,17]. In this study, the CFRP was modelled as a unidirectional fibre in the horizontal direction with a thickness of 0.20 mm.

Table 3. Mechanical properties of CFRP material.

E_1 (GPa)	E_1 (GPa)	G_{12} (GPa)	G_{13} (GPa)	G_{13} (GPa)	ν_{12}
170	90	4.8	4.8	4.8	0.34

Table 4. Parameters used in Hashin failure criteria.

Longitudinal tensile strength (N/mm ²)	Longitudinal compression strength (N/mm ²)	Transverse tensile strength (N/mm ²)	Transverse compressive strength (N/mm ²)	Longitudinal shear strength (N/mm ²)	Longitudinal shear strength (N/mm ²)
2050	1200	62	190	81	81

The geometric properties of composite cylindrical models are listed in table 5, with each model identified with a code ‘C-x-y- θ ’ in which the subcode ‘C’ refers to carbon fibre composite shell, ‘x’ refers to the R/t ratio, ‘y’ refers to L/R ratio, and θ refers to

fibre angle. For instance, C-100-0.5-45 refers to a carbon fibre composite shell model with $R/t = 100$, $L/R = 0.5$ and fibre angle 45/-45.

Table 5. Geometric properties of CFRP composite shells.

Model	Length (mm)	Radius (mm)	Thickness of each layer (mm)	Number of layers	Fiber angle
C-300-0.5-45	150	300	0.2	5	45/-45
C-300-0.5-90	150	300	0.2	5	0/90
C-214-0.5-45	150	300	0.2	7	45/-45
C-214-0.5-90	150	300	0.2	7	0/90
C-100-0.5-45	150	300	0.2	15	45/-45
C-100-0.5-90	150	300	0.2	15	0/90
C-300-1.5-45	300	300	0.2	5	45/-45
C-300-1.5-90	300	300	0.2	5	0/90
C-214-1.5-45	300	300	0.2	7	45/-45
C-214-1.5-90	300	300	0.2	7	0/90
C-100-1.5-45	300	300	0.2	15	45/-45
C-100-1.5-90	300	300	0.2	15	0/90
C-300-3.0-45	600	300	0.2	5	45/-45
C-300-3.0-90	600	300	0.2	5	0/90
C-214-3.0-45	600	300	0.2	7	45/-45
C-214-3.0-90	600	300	0.2	7	0/90
C-100-3.0-45	600	300	0.2	15	45/-45
C-100-3.0-90	600	300	0.2	15	0/90

4. Results and Discussion

In this research, 18 composite shells and 12 steel shells were modelled to investigate the effect of shell material on the buckling behaviour of cylindrical shells and also to evaluate the effect of geometric properties on the buckling load of the shells. The results of the linear and non-linear analyses are presented in tables 6 and 7.

Table 6. Results of the linear and non-linear analyses of steel shells.

Model	Eigenvalue (kPa)	Riks (kPa)	Number of hoop waves
S-300-0.5	312.867	275.274	16
S-300-1.5	99.671	92.999	10
S-300-3	49.343	47.105	7
S-500-0.5	88.000	79.372	19
S-500-1.5	28.123	26.421	11
S-500-3	13.815	13.265	8
S-750-0.5	32.174	29.272	21
S-750-1.5	10.217	9.680	13
S-750-3	5.013	4.835	9
S-1000-0.5	15.827	14.451	22
S-1000-1.5	4.996	4.766	14
S-1000-3	2.453	2.378	10

In figure 3, deformation of buckling waves in composite and steel specimens is shown. The results showed that the magnitude of deformation in composite models is more than steel models, and deformations in composite models are more brittle than steel models.

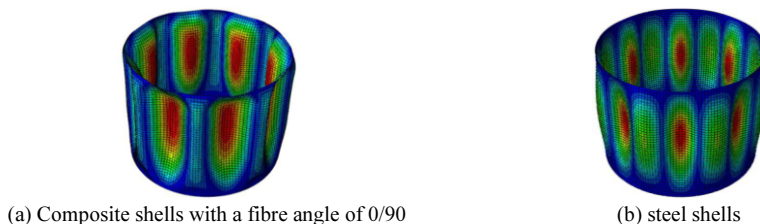


Figure 3. Deformation of buckling waves in composite and steel specimens.

Table 7. Results of the linear and non-linear analyses of CFRP composite shells.

Model	Eigenvalue (kPa)	Riks (kPa)	Number of hoop waves
C-300-0.5-45	84.551	77.401	34
C-300-0.5-90	92.640	85.232	24
C-214-0.5-45	194.663	178.734	30
C-214-0.5-90	210.114	192.418	22
C-100-0.5-45	1140.391	1012.132	26
C-100-0.5-90	1654.301	1492.214	18
C-300-1.5-45	21.966	20.052	18
C-300-1.5-90	38.984	35.692	16
C-214-1.5-45	52.631	46.604	16
C-214-1.5-90	82.154	74.202	14
C-100-1.5-45	381.745	337.101	14
C-100-1.5-90	451.577	397.123	12
C-300-3.0-45	9.971	9.054	14
C-300-3.0-90	21.923	20.848	12
C-214-3.0-45	23.281	21.787	12
C-214-3.0-90	47.150	45.125	12
C-100-3.0-45	164.125	158.241	10
C-100-3.0-90	267.554	242.143	10

In figures 4, 5 and 6, R/t ratio versus external compressive buckling load relationships for cylindrical steel and composite shells with a fibre angle of 45/-45 and 0/90 for various L/R ratios are depicted. The results showed that the buckling capacity decreased with increasing L/R and R/t ratios. Additionally, a non-linear relationship was established between the external R/t ratio and the buckling capacity of the shells.

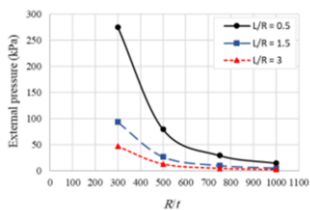


Figure 4. Radius-to-wall thickness vs. external pressure relationships for steel shells with various length-to-radius ratios.

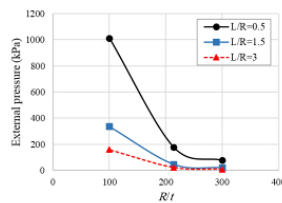


Figure 5. Radius-to-wall thickness vs. external pressure relationships for composite shells with a fibre angle of 45/-45 but various length-to-radius ratios.

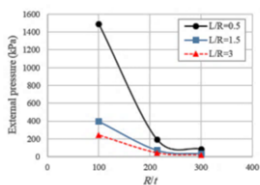


Figure 6. Radius-to-wall thickness vs. external pressure relationships for composite shells with a fibre angle of 0/90 but various length-to-radius ratios.

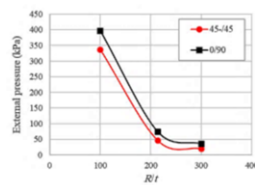


Figure 7. Radius-to-wall thickness vs. external pressure relationships for composite shells with various fibre angles.

In figure 7, the effect of fibre angles on the buckling load of composite shells with a slenderness ratio of $L/R = 1.5$ is investigated. It can be seen that composite shells with fibre angles of 0/90 had higher buckling capacity when compared to composite shells with a fibre angle of 45/-45.

The strength-to-weight parameter was used to compare the effect of composite and steel materials on the buckling behaviour of cylindrical shells. Weight is an essential parameter from an economic perspective because it is directly related to the total cost of the tanks. Additionally, weight is a critical parameter in the seismic design of structures. Therefore, by raising the strength-to-weight ratio, the performance of the structures improves. In figure 8, the bar chart of the strength-to-weight ratio for steel and composite shell models with fibre angles of 45/-45 and 90/0 and for different L/R ratios, but the same $R/t=300$ is shown. The results showed composite models had a higher strength-to-weight ratio than steel shells. Also, composite shells with 0/90 fibre angles performed better than those with 45/-45 fibre angles. On the other hand, for a slenderness ratio equal to 3, composite models with a fibre angle of 45/-45 had poor performance than similar steel shells. Therefore, the fibre angle has a crucial influence on the performance of shells from a strength-to-weight perspective.

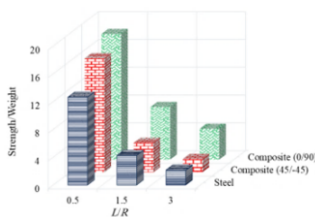


Figure 8. Comparison of strength-to-weight ratio for steel and composite shells with various length-to-radius ratios.

5. Conclusions

In this paper, the effect of steel and composite materials, geometric characteristics of cylindrical shells in the form of radius to thickness ratio (R/t), slenderness ratio (L/R) and fibre angles on the buckling capacity of cylindrical shells when subjected to external pressure were investigated. The results obtained from the conducted research can be summarized as follows:

- (a) For the same radius-to-thickness ratio and thinness ratio, composite shells had a higher strength-to-weight ratio when compared to counterpart steel shells. In addition,

the strength-to-weight ratio of the composite shells with a fibre angle of 0/90 was higher than the counterpart composite shells with a fibre angle of 45/-45.

(b) When the height of a shell is increased while keeping the radius and thickness constant, the buckling load decreases. This indicates an inverse relationship between the buckling load and the L/R ratio. On the other hand, decreasing the R/t ratio for shells with the same radius and height results in an increase in the buckling load.

(c) The magnitude of deformation in composite models is more than steel models, and deformations in composite models are more brittle than steel models.

(d) For the composite shells with the same R/t ratio and thinness, the buckling capacity of the composite shells with a fibre angle of 0/90 was (between 7 and 56%) higher than the counterpart composite cylindrical shells with a fibre angle of 45/-45.

References

- [1] Fazlalipour N, Showkati H, Ghanbari-Ghazijahani T. Experiments on welded shells with section alteration under axial and peripheral pressure. *Journal of Constructional Steel Research*. 2022; 193: 107277.
- [2] Firouzsalar SE, Dizhur D, Jayaraman K, Chouh N, Ingham JM. Flax fabric-reinforced epoxy pipes subjected to lateral compression. *Composite Structures*. 2020; 244: 112307.
- [3] Showkati H, Ansourian P. Influence of primary boundary conditions on the buckling of shallow cylindrical shells. *Journal of Constructional Steel Research*. 1996; 36(1): 53-75.
- [4] Fatemi SM, Showkati H, Maali M. Experiments on imperfect cylindrical shells under uniform external pressure. *Thin-Walled Structures*. 2013; 65: 14-25.
- [5] Maali M, Aydın AC, Showkati H, Fatemi S, Sagioglu M. Longitudinal Imperfections on thin walled cylindrical shells. *J. Civ. Environ. Eng*. 2018; 8: 2-11,
- [6] Pan J, Liang S. Buckling analysis of open-topped steel tanks under external pressure. *SN Applied Sciences*. 2020; 2(4): 535.
- [7] Khatuni SY, Showkati H. Buckling behavior of semi-scale steel tank with carbon fiber reinforced polymer ring subjected to lateral uniform pressure loading. *International Journal of Engineering*. 2019; 32(10): 1407-1415.
- [8] Zhang X, Li Z, Wang P, Pan G. Experimental and numerical analyses on buckling and strength failure of composite cylindrical shells under hydrostatic pressure. *Ocean Engineering*. 2022; 249: 110871.
- [9] Wei R, Shen K, Pan G. A numerical study on the effect of delamination on composite cylindrical shells subjected to hydrostatic pressure. *Ocean Engineering*. 2022; 262: 112294.
- [10] Showkati H, Pashaie TA. Investigation on the Buckling Behavior of GFRP Thin-walled Cylindrical Shells under External Pressure. 2022,
- [11] Hibbitt K. ABAQUS/standard user's manual; ABAQUS/CAE user's manual; ABAQUS keywords manual; ABAQUS theory manual; ABAQUS example problems manual; ABAQUS benchmarks manual; ABAQUS verification manual. 2005, USA: HSK Corporation.
- [12] Fazlalipour N, Showkati H. Geometric properties and imperfections influence on buckling behavior of Variable-Thickness steel cylindrical shells subjected to combined Loading: Experimental and numerical study. *Structures*. 2023; 55: 834-852.
- [13] Fazlalipour N, Showkati H, Firouzsalar SE. Buckling behaviour of cylindrical shells with stepwise wall thickness subjected to combined axial compression and external pressure. *Thin-Walled Structures*. 2021; 167: 108195.
- [14] Fazlalipour N, Showkati H. Experimental and theoretical study of buckling behavior of steel cylindrical shells with variable wall thicknesses under combined loading of axial compression and external pressure. *Sharif Journal of Civil Engineering*. 2022; 38(1.2): 169-177.
- [15] Ghalghachi RN, Showkati H, Firouzsalar SE. Buckling behaviour of GFRP cylindrical shells subjected to axial compression load. *Composite Structures*. 2021; 260: 113269.
- [16] Fazlalipour N, Ghalghachi RN, Firouzsalar SE. Buckling Behaviour of Locally Dented GFRP Cylindrical Shells Under External Pressure—A Numerical Study. *International Conference on Innovative Solutions in Hydropower Engineering and Civil Engineering*; 2022, Springer Nature Singapore Singapore. p. 263-271.
- [17] Naseri R, Showkati H. Experimental and numerical investigation of fracture and buckling behavior of chopped GFRP cylindrical shells subjected to axial compression load. *Sharif Journal of Civil Engineering*. 2021; 37(3.1): 125-134.